Computer Simulation Study of Fullerene Translocation Through Lipid Membranes

Article *in* Nature Nanotechnology · June 2008

DOI: 10.1038/nnano.2008.130 · Source: PubMed

6 authors, including:

Jirasak Wong-ekkabut
Kasetsart University
57 PUBLICATIONS **1,212** CITATIONS

SEE PROFILE

Wannapong Triampo
Mahidol University
132 PUBLICATIONS **1,571** CITATIONS

SEE PROFILE

I-Ming Tang
Silpakorn University
276 PUBLICATIONS **2,363** CITATIONS

SEE PROFILE

Computer simulation study of fullerene translocation through lipid membranes

JIRASAK WONG-EKKABUT[1,2†], SVETLANA BAOUKINA[1], WANNAPONG TRIAMPO[2,3], I-MING TANG[2,4], D. PETER TIELEMAN[1] AND LUCA MONTICELLI[1*‡]

[1]Department of Biological Sciences, University of Calgary, Calgary, Alberta T2N 1N4, Canada
[2]Department of Physics, Faculty of Science, Mahidol University, Bangkok 10400, Thailand
[3]Center of Excellence for Vectors and Vector-Borne Diseases, Mahidol University at Salaya, Nakhonpathom 73170, Thailand
[4]Center of Nanoscience and Nanotechnology, Mahidol University, Bangkok 10400, Thailand
[†]Present address: Department of Applied Mathematics, University of Western Ontario, London, Ontario, Canada
[‡]Present address: Laboratory of Physics, Helsinki University of Technology, Espoo, Finland
*e-mail: luca.monticelli@gmail.com

Published online: 18 May 2008; doi:10.1038/nnano.2008.130

Recent toxicology studies suggest that nanosized aggregates of fullerene molecules can enter cells and alter their functions, and also cross the blood–brain barrier. However, the mechanisms by which fullerenes penetrate and disrupt cell membranes are still poorly understood. Here we use computer simulations to explore the translocation of fullerene clusters through a model lipid membrane and the effect of high fullerene concentrations on membrane properties. The fullerene molecules rapidly aggregate in water but disaggregate after entering the membrane interior. The permeation of a solid-like fullerene aggregate into the lipid bilayer is thermodynamically favoured and occurs on the microsecond timescale. High concentrations of fullerene induce changes in the structural and elastic properties of the lipid bilayer, but these are not large enough to mechanically damage the membrane. Our results suggest that mechanical damage is an unlikely mechanism for membrane disruption and fullerene toxicity.

The extent of the production and use of nanomaterials is rapidly growing. Carbon nanomaterials, such as fullerenes and nanotubes, are among the most extensively studied nanomaterials. Bulk fullerene production at a scale of tons is already under way[1]. Although the effects of nanoparticles on health and the environment are becoming more of a concern, studies on toxicology and the environmental impact of nanoparticles are still scarce[2]. Inhaled ultrafine carbon particles deposit in the lung[3] and translocate into the brain, especially into the olfactory bulb, by means of the olfactory nerves and the blood[4,5]. Fullerene is soluble in numerous organic solvents and it forms a stable colloidal suspension in water, also known as 'nano-C60'[6,7]. This aggregate has been well characterized experimentally and its size lies between tens and a few hundreds of nanometres[6–9]. Experimental results suggest that, despite their large size, fullerene aggregates can penetrate cells and cross the blood–brain barrier[4]. The mechanism of nano-C60 penetration through a lipid membrane has not yet been established. The mechanism of cell membrane disruption is also not well understood. It has been reported that the toxicity of carbon nanoparticles depends on their solubility in water; for example, the cytotoxicity of pristine fullerene is seven orders of magnitude higher than for functionalized fullerenes with high solubility[10]. It has been recently proposed that fullerene causes cell membrane leakage due to lipid peroxidation[11]. On the other hand, it has also been reported that C60 and water-soluble fullerene derivatives could be used as antioxidants against radical-initiated lipid peroxidation[12], as well as drug carriers[13,14]. The protection from lipid peroxidation was found to be higher for pristine C60 than for water-soluble derivatives[12]. Whether the biological activity of fullerenes is desirable or not, experimental evidence published so far indicates that solubility in the membrane interior is an important determinant of biological activity[5].

In the present study we describe the thermodynamics and mechanism of the permeation of fullerene aggregates through cell membranes, based on computer simulations. Previous simulation studies of nanoparticles have investigated the insertion of individual hydrophobic nanotubes in membranes[15,16] and water transport through carbon nanotubes[17,18]. Although fullerene is known to aggregate in water, simulation studies reported so far have focused on monomeric fullerene and water-soluble derivatives, and include investigations of fullerene solvation in water[19], the interactions between fullerene molecules in vacuum[20] and in water[21], the translocation of monomeric C60 across a lipid bilayer[22] and the interaction between two individual C60 molecules inside a lipid bilayer[23]. Following an earlier approach[24–26], we developed a coarse-grained (CG) model based on experimental partitioning of fullerene between polar and nonpolar phases, which is the main determinant of permeation across a lipid membrane[27]. Our work provides insight into the thermodynamics of fullerene clusters permeation through cell membranes and the effect of high concentrations of fullerene on the structural and elastic properties of a lipid bilayer, and suggests that mechanical damage is not likely to be responsible for membrane disruption and fullerene toxicity.

MECHANISM AND ENERGETICS OF FULLERENE PERMEATION

Fullerene is not soluble in water and only marginally soluble in polar organic solvents, but its solubility in hydrocarbons is

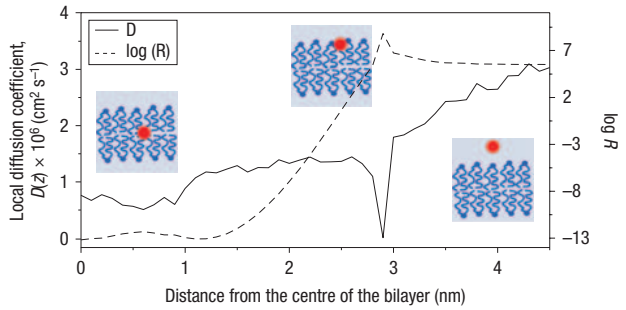

Figure 1 Kinetics of fullerene permeation. Local diffusion coefficient $D(z)$ and local resistance $R(z)$ of fullerene at different depths in a DOPC lipid bilayer. In the insets, the position of fullerene (red sphere) relative to the lipid bilayer (blue) is shown. The permeability of fullerene is higher than for water but much lower than for benzene and other small hydrophobic molecules.

high[28]. Because of its hydrophobic character, fullerene is expected to partition mainly into the lipid bilayer interior, as has been shown previously using atomistic simulations[22]. This is confirmed by calculations of the potential of mean force (PMF) of monomeric fullerene as a function of distance from the centre of the lipid bilayer (see Supplementary Information, Fig. S1). The results show qualitative agreement with atomistic studies[22], although the coarse-grained model suggests that fullerene has an even stronger preference for the bilayer interior.

To characterize the dynamics of fullerene penetration into the bilayer, we calculated the local diffusion coefficients along the bilayer normal $D(z)$ and the local resistances $R(z)$ (Fig. 1). Fullerene diffuses in the bilayer more slowly than in bulk water. The local diffusion coefficients for fullerene are about one order of magnitude less than for small molecules[27,29]. The diffusion rate drops by over an order of magnitude in the head group region. Fullerene permeability is 6×10^{-2} cm s^{-1} at 300 K, higher than for water[30] and about two orders of magnitude lower than for benzene[29].

Unbiased simulations confirm that monomeric fullerene placed in bulk water spontaneously enters the bilayer within a few hundred nanoseconds. Fullerene rapidly passes the lipid head group region (average time, ~500 ps) and then moves more slowly towards the lipid tails region (Fig. 2a). Inside the bilayer, it dwells within about 1 nm of the centre and translocation outside is never observed, consistent with the large energy barrier for transfer from the bilayer to water. We performed additional simulations of fullerene permeation in a dipalmitoylphosphatidylcholine (DPPC) lipid bilayer. Translocation kinetics and thermodynamics did not show significant differences between the two model membranes (see Supplementary Information).

To investigate fullerene aggregation and its effect on permeability, we performed 22 simulations (4 μs each) of a large dioleoylphosphatidylcholine (DOPC) bilayer with 16 fullerenes. Fullerene molecules were initially placed either close to the centre (5 simulations), close to the lipid head group region (5 simulations) or in bulk water (12 simulations). In the water phase, fullerenes aggregated into a large cluster within hundreds of nanoseconds. In two simulations the clusters included all 16 molecules and did not penetrate the membrane within the simulation time. In all other cases (10 simulations), smaller clusters of up to ten molecules formed, which penetrated the bilayer (Fig. 2b). The average waiting time for the penetration of fullerene aggregates in the bilayer was ~1 μs. The first step of fullerene translocation is the formation of a small pore in the lipid head group region. This free space is readily filled by one fullerene (protruding from the aggregate; Fig. 2b, 768 ns). Averaging over ten simulations, the lifetime of the pore is less than 500 ps. The pore does not appear to be induced by the proximity of the fullerene cluster; nanoparticles were found within 0.6 nm of the lipid head group region several times in each simulation before translocation occurred. Instead, local area fluctuations in the bilayer play an important role in the penetration mechanism. After the first fullerene is inserted in the head group region, it readily moves towards the lipid tail region, followed by the rest of the cluster (which does not substantially change its geometry). As the lipid head groups move aside to make room for the fullerene cluster, no free space pockets are formed. A cluster of ten fullerenes requires ~15 ns to completely pass the lipid head groups, compared with ~500 ps for monomeric fullerene.

When fullerenes are placed close to the lipid head group region, only small clusters (two or three molecules) form rapidly and penetrate the bilayer within a few hundred nanoseconds. After penetration, they disaggregate on a microsecond timescale. When fullerenes are placed inside the bilayer, they do not form stable aggregates.

It is known that fullerene in water spontaneously forms nanosized aggregates[6–8]. Therefore, it is important to evaluate the energetic balance for its transfer from an aggregate in water to a position inside the bilayer. For computational reasons, we started from a solid-like (periodic) fullerene aggregate and calculated the energy required to move a single fullerene from the aggregate into the gas phase. We then calculated the hydration free energy (for a single fullerene), corresponding to the transfer from the gas phase into bulk water, and finally the free energy of transfer from bulk water into the centre of the lipid bilayer. These artificial steps combined describe the full process of interest. Transferring one fullerene from the aggregated form into bulk water is highly unfavourable, with a free energy cost of 60 ± 20 kJ mol^{-1}. The energy gain upon transfer from bulk water to the bilayer interior is 110 kJ mol^{-1}. Summing the contributions, the overall balance indicates that removing one fullerene from a large fullerene aggregate and placing it into the bilayer interior is favourable by 50 ± 20 kJ mol^{-1}. This result is consistent with our unbiased simulations, showing that fullerene clusters spontaneously penetrate the lipid bilayer.

EFFECT OF FULLERENE ON THE LIPID MEMBRANE

The perturbation of bilayer properties upon insertion of a single fullerene molecule was calculated in bilayers of two sizes using biased molecular dynamics (MD) simulations, in which fullerene was restrained at different positions along the bilayer normal. Despite the large size of fullerene, perturbation of the bilayer structure is relatively small; bilayer thickness, area per lipid and lipid order parameters change only slightly upon fullerene insertion (Fig. 3). The deformations are largest when fullerene is found between 1.5 and 2.9 nm from the centre of the bilayer. However, even in the smallest bilayer, the area decreases by less than 2% during fullerene permeation. The increase in bilayer thickness and in the ordering of the lipid tails are also minor. These structural changes can be explained by the appearance of lipid protrusions when fullerene is inserted in the head group and carbonyl regions. As the lipids close to fullerene protrude towards the water phase, their tails stretch and become more ordered. This, in turn, reduces the area and increases the thickness of the membrane. Structural

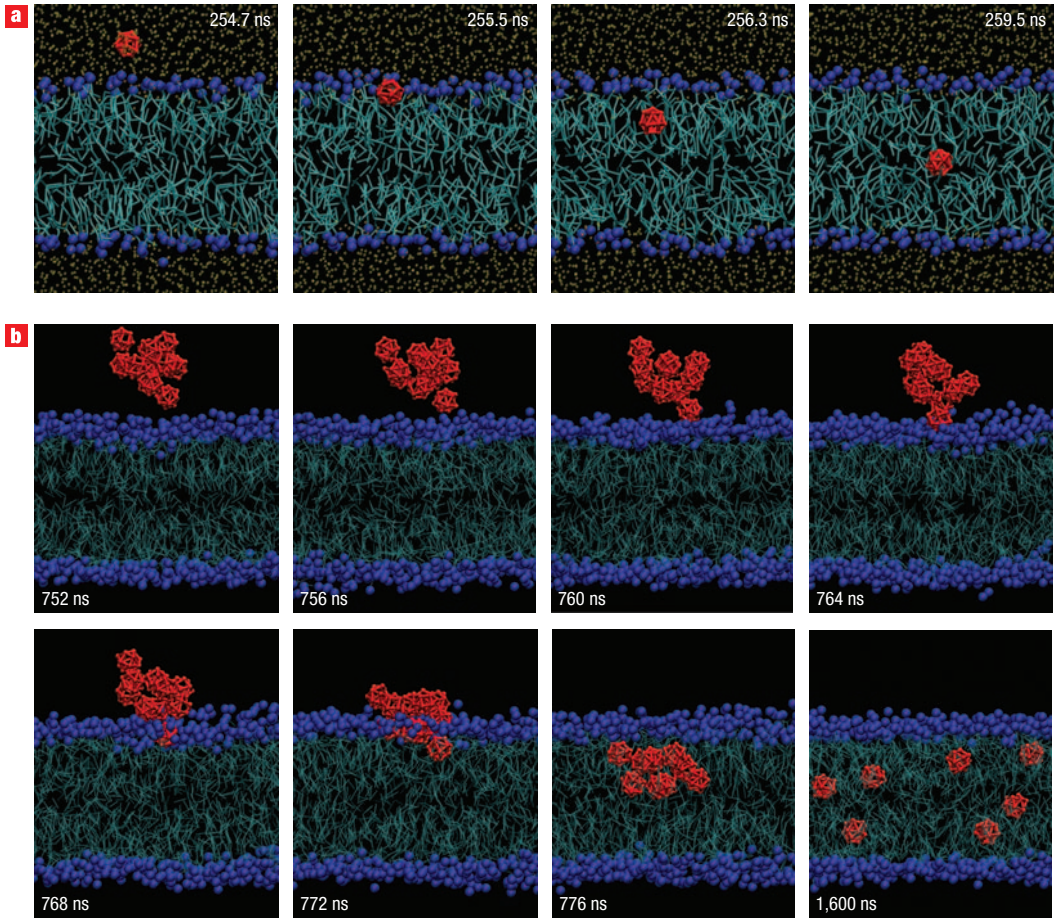

Figure 2 Mechanism of permeation of fullerene through a lipid membrane. a, Monomeric fullerene rapidly crosses the lipid head group region, then diffuses more slowly in the membrane interior. Fullerene is shown in red, the lipids in cyan with blue head groups (phosphodiester groups), and water is yellow. The simulation time is indicated in each snapshot. **b**, Penetration of a cluster of ten fullerenes. Lipid phosphodiester groups are shown as blue spheres, lipid tails as cyan lines; water is not represented. The permeation of fullerene clusters is much slower than for monomers, and starts with the insertion of a single fullerene in the lipid head group region. The simulation time is indicated in each snapshot.

modifications are smaller in the largest bilayer (data not shown). Significant curvature of the bilayer is observed, and lipid protrusions are not observed.

To test the effect of higher fullerene concentrations on the properties of the membrane, we performed simulations of a large lipid bilayer (1,152 DOPC molecules) in the absence of nanoparticles and with fullerene:DOPC ratios of 1:72, 1:18 and 1:9 (molar fractions: 1.4%, 5.5% and 11.1%). The initial position of fullerene molecules was chosen randomly within 3.5 nm from the bilayer centre, so most fullerenes were inside the membrane (or close to it) at the beginning of the simulations. We performed three simulations at each concentration, each for 4 μs. All fullerene molecules penetrated the bilayer in each simulation. Even at the highest concentration, we did not observe the formation of stable aggregates inside the bilayer on the simulation timescale (see Fig. 4a). Fullerenes are most often found 0.5–1 nm displaced from the centre (Fig. 4b).

Because of the relatively large size of fullerene (diameter of ~1 nm), its displacement from the centre of the bilayer induces asymmetry in the membrane, leading to transient distortions, both in-plane and out-of-plane. These deformations include area stretching, bilayer thickening, individual lipid protrusions and bilayer bending. In order to quantify these deformations, we calculated different structural, dynamic and elastic properties of the membrane as a function of fullerene concentration (Table 1). As the nanoparticle concentration increases, we observe an increase in both the projected area and the thickness of the bilayer. At the highest ratio, the area per lipid increases by 4% and the bilayer thickness by 2.7%. Analysis of the order parameter of the bonds in the lipid tails shows that even the highest concentration of nanoparticles has a negligible effect on lipid chain order. On the other hand, dynamic and elastic properties of the bilayer are affected by the nanoparticles to a larger extent. The lipid diffusion coefficient decreases with increasing fullerene concentration in an approximately linear fashion. For DOPC lipids in the absence of fullerene, the diffusion coefficient (1.0×10^{-7} cm^2 s^{-1}) is in excellent agreement with experiment[31]. The bending modulus of the pure DOPC bilayer is $(5.5 \pm 1.0) \times 10^{-20}$ J, close to values previously reported for DPPC bilayers[24] (4×10^{-20} J) and to experimental data by Evans and co-workers[32] (8.5×10^{-20} J). A fullerene concentration of 11.1% reduces the lateral diffusion coefficients by ~40%, the area compressibility modulus by less than 10% and the bending modulus by ~20%. The decrease in both elastic

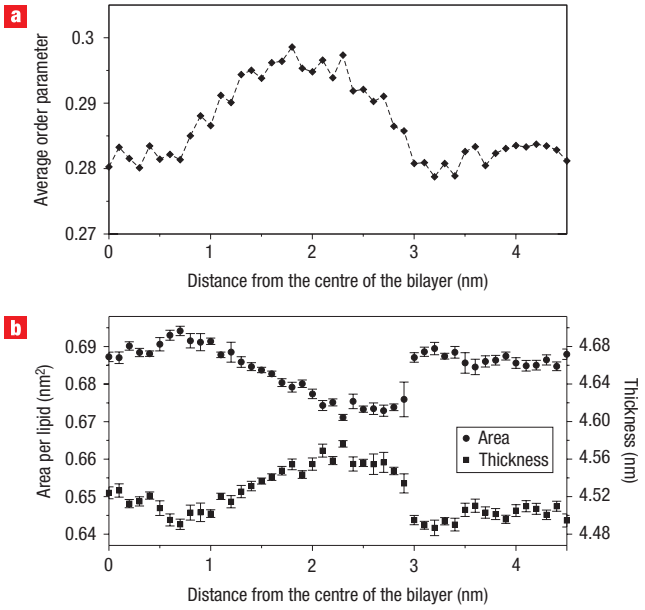

Figure 3 Structural properties of the membrane during fullerene permeation. a, Average order parameter of the lipid tails as a function of the distance of fullerene from the centre of the bilayer. **b**, Area per lipid and thickness of the lipid bilayer as a function of the distance between fullerene and the centre of the bilayer. Vertical bars represent standard deviations. The area per lipid was not corrected for the presence of the nanoparticle. The perturbation of membrane structural properties is minor.

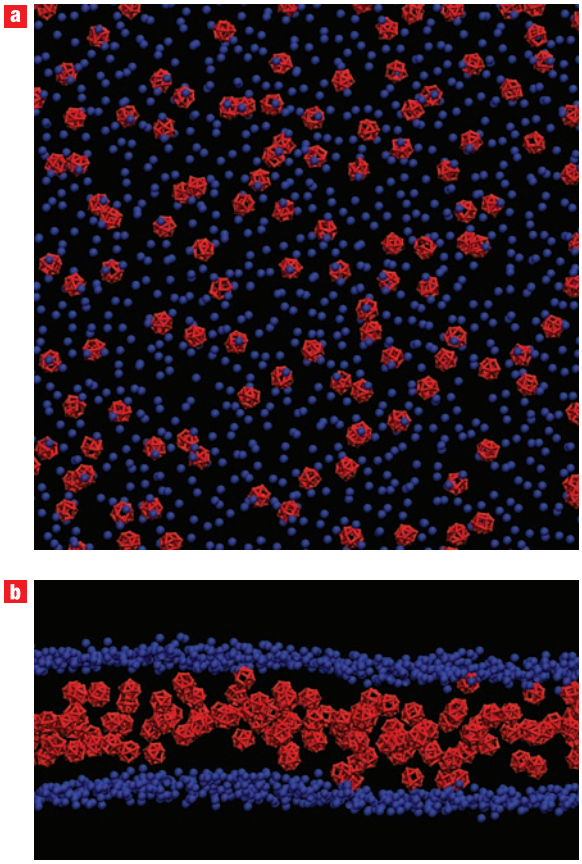

Figure 4 Distribution of fullerene in the membrane. Snapshots are taken from a simulation with 128 fullerenes and 1,152 DOPC lipids, after 4 μs of simulation. Phosphate groups are shown as blue spheres, fullerenes are in red; lipid tails and water are not shown for clarity. **a**, Top view, showing the lateral distribution of fullerene in the membrane. Even at very large concentrations, fullerenes do not form aggregates in the membrane. **b**, Side view, showing the distribution of fullerene along the membrane normal.

moduli indicates a slight softening of the membrane. However, no noticeable mechanical damage (bilayer rupture, micellization, formation of pores) occurred within the simulation time.

DISCUSSION

It has been reported in the literature that carbon nanoparticles can pass through the blood–brain barrier and translocate into the brain and the olfactory bulb[8]. Our simulations show that fullerene clusters can easily penetrate into a lipid membrane by means of passive transport. Considering the overall thermodynamic balance for the transfer of fullerene from an aggregate into the membrane interior, the value of -50 ± 20 kJ mol^{-1} indicates that the process is spontaneous.

Both the free energy of fullerene translocation (from water to the membrane) and its kinetics are similar in DOPC and DPPC membranes, suggesting that the main conclusions of our study are only weakly dependent on the nature of the lipid tails. The time required for monomeric fullerene to completely pass the head group region is ~500 ps, on the same timescale of 70–160 ps as in previously reported atomistic simulations[22]. Compared with such simulations[22], the PMF, however, is significantly different; atomistic simulations gave a total stabilization of $\sim 35 \pm 8$ kJ mol^{-1}. On the other hand, the position of the energy minimum (~1 nm from the centre of the membrane) is in excellent agreement. Deviations from atomistic results can be ascribed to differences in the details of the force fields and insufficient sampling in atomistic simulations due to prohibitively high computational cost.

The mechanism of permeation for fullerene clusters is similar to that for the monomer, with small pores being formed in the lipid head group region immediately before penetration and being rapidly filled by one nanoparticle. On the other hand, the kinetics is significantly slower, with both waiting times and penetration times about one order of magnitude longer in the case of aggregates. Translocation of fullerene clusters is observed on a timescale of microseconds, a relatively short time for biological processes. The formation of pockets of free volume sufficiently large to accommodate a fullerene molecule is a rare event and depends on local area fluctuations, not on the presence of fullerene. The head group region of lipid bilayers is very polar and highly hydrated. Free volume pockets have a short lifetime and do not reach the lipid tail region, so they do not disrupt the hydrophobic barrier represented by the lipid membrane.

Fullerene differs from some small hydrophobic molecules[27] in that it does not show a preference for the centre of the bilayer and is more often found displaced (~1 nm) from the centre. The preference of fullerene for a region at 1 nm distance from the centre of the bilayer has also been observed previously in atomistic simulations[22], although in that case the preference was stronger (~20 kJ mol^{-1} relative to the bilayer centre). This tendency can be explained as the result of opposing forces; the large amount of accessible free volume[27] and the minimal perturbation of the bilayer structure drive fullerene towards the centre, and the higher number of dispersion interactions favours displacement towards a denser region of the bilayer.

Table 1 Structural, dynamic and elastic properties of DOPC lipid bilayers at different fullerene concentrations. Results are the average over three independent simulations (±error estimate).

	Fullerene concentration (molar)			
	0%	1.4%	5.5%	11.1%
Area per lipid (nm^2)	0.669 ± 0.004	0.673 ± 0.004	0.683 ± 0.004	0.697 ± 0.004
Thickness (nm)	4.30 ± 0.09	4.43 ± 0.02	4.46 ± 0.01	4.53 ± 0.01
Average order parameter	0.283 ± 0.001	0.283 ± 0.001	0.283 ± 0.001	0.284 ± 0.001
D ($\times 10^7$ cm^2 s^{-1})*	1.01 ± 0.03	0.98 ± 0.03	0.77 ± 0.03	0.62 ± 0.02
K_A ($\times 10^{-3}$ N m^{-1})†	371 ± 8	364 ± 8	365 ± 5	346 ± 9
k_C ($\times 10^{-20}$ J)‡	5.5 ± 1.0	5.1 ± 1.2	4.9 ± 0.6	4.4 ± 0.6

*Self-diffusion coefficient of DOPC lipids.
†Area compressibility modulus of the bilayer.
‡Bending modulus of the bilayer.

Table 2 Free energy of transfer of fullerene between organic solvents (in kJ mol^{-1}).

	Benzene	Cyclohexane	Acetone
ΔG (calculated)			
Benzene	—	—	—
Cyclohexane	−4.1 ± 2.8	—	—
Acetone	−10.2 ± 2.3	−5.1 ± 1.9	—
Ethanol	−19.5 ± 2.3	−15.4 ± 2.0	−10.3 ± 1.0
ΔG (experimental)[28]			
Benzene	—	—	—
Cyclohexane	−12.1	—	—
Acetone	−18.5	−6.4	—
Ethanol	−22.5	−10.4	−4.0
$\Delta\Delta G$ (expt−calc)			
Benzene	—	—	—
Cyclohexane	−8.0	—	—
Acetone	−8.3	−1.4	—
Ethanol	−3.0	5.0	6.3

The formation of stable aggregates inside the bilayer was not observed on the simulation timescale. This observation is consistent with other atomistic simulations showing that interactions between two C60 molecules in a lipid bilayer are repulsive at short distances[23].

The deformations induced by fullerene on the lipid membrane depend on its concentration. High loads of fullerene affect the structural, elastic and dynamic properties of the bilayer. The bilayer thickness is increased, in qualitative agreement with experimental results on multilamellar oriented bilayers[33], but lipid diffusion becomes slower and the bilayer becomes more flexible. The magnitude of these effects is comparable to reduced diffusion by the addition of cholesterol[31] and increased flexibility by the addition of moderate concentrations of short-chain alcohols[34] or lysolipids[35]. Larger changes in membrane flexibility have been observed in lipid bilayers with two unsaturations per acyl tail or with shorter acyl tails[32]. More sizeable effects on dynamic and elastic properties have also been predicted for lipid rafts[36]. In all the cases mentioned above, modifications of dynamic and elastic properties did not lead to membrane disruption. Moreover, no indication of membrane instability was found in our simulations. Therefore our results suggest that the presence of fullerene at a high concentration is unlikely to result in mechanical damage to lipid membranes.

Changes in cell membrane elasticity can alter cellular functions by modifying the properties and functioning of membrane proteins. Activation of some membrane proteins has been shown to depend on the elastic properties of the membrane, which in turn depend on membrane composition (for recent reviews, see refs 37 and 38). This mechanism does not imply membrane disruption. It is reasonable to expect that fullerene permeation would affect cell function by changing the elastic properties of cell membranes. Another possible mechanism for fullerene biological activity had been proposed recently based on the active radical chemistry of fullerene. Some earlier studies have indicated that the toxicity of nanosized fullerene aggregates is due to lipid peroxidation[11], but elsewhere it has been found that C60 can act as an antioxidant against radical-initiated lipid peroxidation[12]. Because fullerene is found preferably in the lipid tail region, close to the double bonds (which are susceptible to peroxidation), our observations are compatible with these findings. Finally, it is possible that fullerene interacts directly with other components of cell membranes, including other lipids, carbohydrates and proteins that are not considered in our simulations.

In summary, we investigated the thermodynamics and the kinetics of fullerene translocation into lipid bilayers using molecular dynamics simulations. Although fullerenes rapidly aggregate in water, they do not aggregate in the bilayer at high concentrations of up to one fullerene per nine lipids. Both monomeric and oligomeric fullerenes penetrate easily in DOPC lipid bilayers on the microsecond timescale. Once inside the bilayer, fullerene clusters disaggregate on a timescale of hundreds of nanoseconds. Free energy calculations indicate that although dissolving a fullerene aggregate in water presents a high energetic cost, the energy gain of transferring fullerene inside a lipid bilayer is higher, so the balance of the overall process is thermodynamically favourable. Upon penetration, fullerene induces small distortions in the structure of the bilayer and a modest increase in membrane softness. Our results suggest that even high concentrations of fullerene are unlikely to cause mechanical damage to the membrane.

METHODS

COARSE-GRAINED FORCE FIELD CALIBRATION

Coarse-grained models allow systems to be studied on longer time- and length-scales than more detailed atomistic models. We built CG models for fullerene compatible with the MARTINI CG force field for lipids and proteins developed by Marrink[24–26]. Parameters for the lipids were taken from the MARTINI force field[25]. Based on comparison of diffusion constants in CG and atomistic simulations, the effective time sampled using our CG model is larger than the formal simulation time, and a similar scaling factor applies to all molecules in the simulated systems[24,25]. In the rest of the paper we use an effective time, instead of the formal simulation time, and the conversion factor is a factor of four.

The fullerene model consists of 16 particles, with an approximate 4:1 mapping of the atoms onto CG beads. The solubility of fullerene in water is extremely low and currently not measurable accurately[39], so free energies of hydration or partitioning into water are not available experimentally. Therefore, we parameterized the non-bonded interactions based on the free energy of transfer of fullerene between polar (ethanol and acetone) and apolar (benzene and cyclohexane) solvents. Free energies were calculated using the

thermodynamic integration technique (see Supplementary Information for details of the methods), and are reported in Table 2 together with experimental transfer of free energies. According to solubility measurements[28,39], transferring fullerene from acetone to cyclohexane implies a gain in energy of 6.45 kJ mol^{-1}. In the case of our model, we found a value of 5.1 kJ mol^{-1}, in good agreement with experimental results. Differences between experimental and calculated free energies of transfer were less than 9 kJ mol^{-1} in all cases. Although there is clearly room for improvement of the force field, the agreement with experimental partitioning data is reasonable.

MOLECULAR DYNAMICS SIMULATIONS

Molecular dynamics simulations of monomeric fullerene were carried out in a water/DOPC system at 300 K and in a water/DPPC system at 325 K. We placed a single fullerene at different distances from the centre of the bilayer and used harmonic restraints on the fullerene for 40 ns to allow for equilibration of the solvent and the lipids. The restraints were then released and five simulations (with different initial velocities) were run in DOPC (and two additional ones in DPPC) for 4 μs each, for a total (production) simulation time of 28 μs.

Simulations of fullerene aggregation were performed both in water and in a DOPC bilayer. Sixteen fullerene molecules were placed at different distances from the centre of the bilayer, corresponding to (a) the bulk water phase, (b) the interface and (c) the bilayer interior. Five simulations were performed (using different seed numbers for the generation of the initial velocities) with fullerenes inside the bilayer, five with fullerenes at the lipid/water interface, twelve with fullerenes in bulk water. Each simulation was carried out for 4 μs, for a total simulation time of 88 μs.

Properties of the DOPC membrane were calculated from a separate set of simulations on systems containing 1,152 lipids. Three simulations were carried out for each fullerene ratio (no fullerene, 1:72, 1:18 and 1:9), each 4 μs long, for a total simulation time of 48 μs.

FREE ENERGY CALCULATIONS

The thermodynamic integration method was used to calculate the free energy of transfer of one fullerene from a fullerene aggregate containing 512 fullerene molecules into the gas phase, and from the gas phase into water. The PMF of fullerene as a function of the distance from the centre of a DOPC lipid bilayer was calculated using the umbrella sampling technique[40] and the weighted histogram analysis method (WHAM)[41]. The calculation of fullerene permeability through lipid bilayers was performed using constraint simulations, using previously described methods[27,42]. All simulations were carried out at constant temperature (300 K) and with semi-isotropic pressure coupling, allowing for changes in the box size in all dimensions. Additional PMF calculations were performed in a DPPC bilayer at 325 K, using identical methodology and simulation parameters. All simulations were run using GROMACS 3.3.1 (ref. 43).

Received 15 February 2008; accepted 21 April 2008; published 18 May 2008.

References

1. Murayama, H., Tomonoh, S., Alford, J. M. & Karpuk, M. E. Fullerene production in tons and more: From science to industry. *Fuller. Nanotub. Carbon Nanostruct.* **12,** 1–9 (2004).
2. Colvin, V. L. The potential environmental impact of engineered nanomaterials. *Nature Biotechnol.* **21,** 1166–1170 (2003).
3. Oberdorster, G., Ferin, J. & Lehnert, B. E. Correlation between particle size, *in vivo* particle persistence, and lung injury. *Environ. Health Perspect.* **102** (suppl. 5), 173–179 (1994).
4. Oberdorster, G. *et al.* Translocation of inhaled ultrafine particles to the brain. *Inhal. Toxicol.* **16,** 437–445 (2004).
5. Oberdorster, G., Oberdorster, E. & Oberdorster, J. Nanotoxicology: an emerging discipline evolving from studies of ultrafine particles. *Environ. Health Perspect.* **113,** 823–839 (2005).
6. Fortner, J. D. *et al.* C-60 in water: Nanocrystal formation and microbial response. *Environ. Sci. Technol.* **39,** 4307–4316 (2005).
7. Lyon, D. Y., Adams, L. K., Falkner, J. C. & Alvarez, P. J. J. Antibacterial activity of fullerene water suspensions: Effects of preparation method and particle size. *Environ. Sci. Technol.* **40,** 4360–4366 (2006).
8. Oberdorster, E. Manufactured nanomaterials (fullerenes, C60) induce oxidative stress in the brain of juvenile largemouth bass. *Environ. Health Perspect.* **112,** 1058–1062 (2004).
9. Andrievsky, G., Klochkov, V. & Derevyanchenko, L. Is the C-60 fullerene molecule toxic? *Fuller. Nanotub. Carbon Nanostruct.* **13,** 363–376 (2005).
10. Sayes, C. M. *et al.* The differential cytotoxicity of water-soluble fullerenes. *Nano Lett.* **4,** 1881–1887 (2004).
11. Sayes, C. M. *et al.* Nano-C60 cytotoxicity is due to lipid peroxidation. *Biomaterials* **26,** 7587–7595 (2005).
12. Wang, I. C. *et al.* C-60 and water-soluble fullerene derivatives as antioxidants against radical-initiated lipid peroxidation. *J. Med. Chem.* **42,** 4614–4620 (1999).
13. Foley, S. *et al.* Cellular localisation of a water-soluble fullerene derivative. *Biochem. Biophys. Res. Commun.* **294,** 116–119 (2002).
14. Venkatesan, N., Yoshimitsu, J., Ito, Y., Shibata, N. & Takada, K. Liquid filled nanoparticles as a drug delivery tool for protein therapeutics. *Biomaterials* **26,** 7154–7163 (2005).
15. Lopez, C. F., Nielsen, S. O., Moore, P. B. & Klein, M. L. Understanding nature's design for a nanosyringe. *Proc. Natl Acad. Sci. USA* **101,** 4431–4434 (2004).
16. Srinivas, G. & Klein, M. L. Computational approaches to nanobiotechnology: probing the interaction of synthetic molecules with phospholipid bilayers via a coarse grain model. *Nanotechnology* **15,** 1289–1295 (2004).
17. Beckstein, O. & Sansom, M. S. Liquid–vapor oscillations of water in hydrophobic nanopores. *Proc. Natl Acad. Sci. USA* **100,** 7063–7068 (2003).
18. Hummer, G., Rasaiah, J. C. & Noworyta, J. P. Water conduction through the hydrophobic channel of a carbon nanotube. *Nature* **414,** 188–190 (2001).
19. Choudhury, N. A molecular dynamics simulation study of buckyballs in water: atomistic versus coarse-grained models of C60. *J. Chem. Phys.* **125,** 034502 (2006).
20. Izvekov, S., Violi, A. & Voth, G. A. Systematic coarse-graining of nanoparticle interactions in molecular dynamics simulation. *J. Phys. Chem. B* **109,** 17019–17024 (2005).
21. Li, L., Bedrov, D. & Smith, G. D. Repulsive solvent-induced interaction between C60 fullerenes in water. *Phys. Rev. E* **71,** 011502 (2005).
22. Qiao, R., Roberts, A. P., Mount, A. S., Klaine, S. J. & Ke, P. C. Translocation of C60 and its derivatives across a lipid bilayer. *Nano Lett.* **7,** 614–619 (2007).
23. Li, L., Davande, H., Bedrov, D. & Smith, G. D. A molecular dynamics simulation study of C60 fullerenes inside a dimyristoylphosphatidylcholine lipid bilayer. *J. Phys. Chem. B* **111,** 4067–4072 (2007).
24. Marrink, S. J., de Vries, A. H. & Mark, A. E. Coarse grained model for semiquantitative lipid simulations. *J. Phys. Chem. B* **108,** 750–760 (2004).
25. Marrink, S. J., Risselada, H. J., Yefimov, S., Tieleman, D. P. & de Vries, A. H. The MARTINI forcefield: coarse grained model for biomolecular simulations. *J. Phys. Chem. B* **111,** 7812–7824 (2007).
26. Monticelli, L. *et al.* The MARTINI coarse-grained force field: extension to proteins. *J. Chem. Theory Comput.*, doi: 10.1021/ct700324x.
27. Marrink, S. J. & Berendsen, H. J. C. Permeation process of small molecules across lipid membranes studied by molecular dynamics simulations. *J. Phys. Chem.* **100,** 16729–16738 (1996).
28. Ruoff, R. S., Tse, D. S., Malhotra, R. & Lorents, D. C. Solubility of C60 in a variety of solvents. *J. Phys. Chem.* **97,** 3379–3383 (1993).
29. Bemporad, D., Essex, J. W. & Luttmann, C. Permeation of small molecules through a lipid bilayer: A computer simulation study. *J. Phys. Chem. B* **108,** 4875–4884 (2004).
30. Paula, S., Volkov, A. G., VanHoek, A. N., Haines, T. H. & Deamer, D. W. Permeation of protons, potassium ions, and small polar molecules through phospholipid bilayers as a function of membrane thickness. *Biophys. J.* **70,** 339–348 (1996).
31. Filippov, A., Oradd, G. & Lindblom, G. The effect of cholesterol on the lateral diffusion of phospholipids in oriented bilayers. *Biophys. J.* **84,** 3079–3086 (2003).
32. Rawicz, W., Olbrich, K. C., McIntosh, T., Needham, D. & Evans, E. Effect of chain length and unsaturation on elasticity of lipid bilayers. *Biophys. J.* **79,** 328–339 (2000).
33. Jeng, U. S. *et al.* Dispersion of fullerenes in phospholipid bilayers and the subsequent phase changes in the host bilayers. *Physica B* **357,** 193–198 (2005).
34. Ly, H. V. & Longo, M. L. The influence of short-chain alcohols on interfacial tension, mechanical properties, area/molecule, and permeability of fluid lipid bilayers. *Biophys. J.* **87,** 1013–1033 (2004).
35. Brown, M. F., Thurmond, R. L., Dodd, S. W., Otten, D. & Beyer, K. Elastic deformation of membrane bilayers probed by deuterium NMR relaxation. *J. Am. Chem. Soc.* **124,** 8471–8484 (2002).
36. Niemelä, P. S., Ollila, S., Hyvonen, M. T., Karttunen, M. & Vattulainen, I. Assessing the nature of lipid raft membranes. *PLoS Comput. Biol.* **3,** 304–312 (2007).
37. Lundbaek, J. A. Regulation of membrane protein function by lipid bilayer elasticity—a single molecule technology to measure the bilayer properties experienced by an embedded protein. *J. Phys. Condens. Matter* **18,** S1305–S1344 (2006).
38. McIntosh, T. J. & Simon, S. A. Roles of bilayer material properties in function and distribution of membrane properties. *Annu. Rev. Biophys. Biomolec. Struct.* **35,** 177–198 (2006).
39. Marcus, Y. *et al.* Solubility of C60 fullerene. *J. Phys. Chem. B* **105,** 2499–2506 (2001).
40. Torrie, G. M. & Valleau, J. P. Nonphysical sampling distribution in Monte Carlo free energy estimation: umbrella sampling. *J. Comput. Phys.* **23,** 187–199 (1977).
41. Kumar, S., Bouzida, D., Swendsen, R. H., Kollman, P. A. & Rosenberg, J. M. The weighted histogram analysis method for free-energy calculations on biomolecules.1. The method. *J. Comp. Chem.* **13,** 1011–1021 (1992).
42. Marrink, S. J. & Berendsen, H. J. C. Simulation of water transport through a lipid membrane. *J. Phys. Chem.* **98,** 4155–4168 (1994).
43. Lindahl, E., Hess, B. & van der Spoel, D. GROMACS 3.0: A package for molecular simulation and trajectory analysis. *J. Mol. Model.* **7,** 306–317 (2001).

Supplementary Information accompanies this paper at www.nature.com/naturenanotechnology.

Acknowledgements

L.M. thanks M.M. Sperotto for fruitful discussions about membrane elasticity theory. This research was supported by the Natural Sciences and Engineering Research Council of Canada (NSERC). J.W. and I-M.T. are supported by the Royal Golden Jubilee PhD Program (PHD/0240/2545). W.T. is supported by the National Center for Genetic Engineering and Biotechnology (BIOTEC) and Thailand Research Fund (TRF). S.B. is an Alberta Ingenuity postdoctoral fellow, D.P.T. is an Alberta Heritage Foundation for Medical Research (AHFMR) Senior Scholar and Canadian Institutes for Health Research New Investigator, and L.M. is an AHFMR postdoctoral fellow. Calculations were performed in part on WestGrid facilities.

Author contributions

L.M. and D.P.T. conceived and designed the simulations. J.W., S.B. and L.M. performed the simulations and analysed the results. W.T., I-M.T. and D.P.T. contributed materials and funding. The paper was written by L.M., with substantial contributions by D.P.T. and J.W. All authors discussed the results and commented on the manuscript.

Author information

Reprints and permission information is available online at http://npg.nature.com/reprintsandpermissions/. Correspondence and requests for materials should be addressed to L.M.